The Sequence-Specific Association of the ETS Domain of Murine PU.1 with DNA Exhibits Unusual Energetics[†]

Gregory M. K. Poon, Petra Gross,[‡] and Robert B. Macgregor, Jr.*

Department of Pharmaceutical Sciences, Faculty of Pharmacy, University of Toronto, Toronto, Ontario M5S 2S2, Canada

Received July 9, 2001; Revised Manuscript Received November 1, 2001

ABSTRACT: PU.1 belongs to the ETS family of transcription factors whose DNA-binding domains recognize purine-rich sequences containing the consensus 5′-GGAA/T-3′. We have characterized the sequence-specific association of the ETS domain of murine PU.1 to the λB site of the Igλ2−4 enhancer as a function of temperature and pH by electrophoretic mobility shift, filter binding, and CD spectroscopy. From 0 to 25 °C, the dissociation equilibrium constant K_D is, within experimental uncertainty, insensitive to temperature, and is only a weak function of temperature from 25 to 52 °C. van't Hoff analysis yielded a small value of $\Delta C_p = -2.1$ kJ mol^{-1} K^{-1} in phosphate buffer, pH 7.4, containing 250 mM Na^+. K_D also shows a weak dependence at 25 °C on pH from 6.7 to 9.0 in phosphate, cacodylate, and Tris buffers that have disparate heats of ionization. The CD spectrum of the protein−DNA complex could be accounted for by a simple linear combination of the spectra of the free components throughout the binding temperature range. Structural calculations indicate that dehydration of solvent-accessible contact surfaces on the protein and DNA accounts for up to $\Delta C_p \sim -1$ kJ mol^{-1} K^{-1}. Taken together, these observations suggest that the hydrophobic effect and, in particular, coupled folding do not contribute significantly to the energetics of sequence-specific association. This is unusual with respect to other sequence-specific protein−DNA interactions for which significant enthalpic contributions and large negative heat capacities are commonly observed.

A common observation in the thermodynamic characterization of sequence-specific protein−DNA association is a large negative change in heat capacity ΔC_p,[1] and, accordingly, strongly temperature-dependent enthalpies and entropies of association (*1*−*13*). While a variety of processes can produce this pattern (*14, 15*), it is generally explained in terms of the hydrophobic effect (*16*). The molecular origin of the hydrophobic effect is usually attributed to protein folding coupled to site-specific DNA binding (*13, 17*) resulting in dehydration of significant amounts of solvent-exposed hydrophobic protein surfaces with an attendant (entropically favorable) release of thermodynamically bound water molecules into the bulk solvent. Efforts to estimate the relative contributions to the free energy of association by dissection of the observed entropy of association point to the hydrophobic effect as the major favorable contributor to binding (*17, 18*), a theme reproduced from earlier studies on the thermodynamic stability of globular proteins (*19*).

Coupled folding has also been proposed as a means of achieving sequence specificity (*17*), whereby a portion of the binding energy is channelled into inducing steric complementarity between the binding surfaces on the protein and DNA by means of coupled folding (*18*). This is consistent with, for example, a near-zero ΔC_p found for nonspecific Cro−DNA association (*12*), the predominantly electrostatic nature of nonspecific DNA binding by the RNA polymerase holoenzyme (*20*) and model oligopeptides (*21, 22*), as well as the greater number of thermodynamically bound water molecules released in the sequence-specific *Eco*RI−DNA complex vs the nonspecific one (*23, 24*).

The PU.1 protein is a member of the ETS family of transcription factors. The ETS domain unites a large number of regulatory proteins that are found in viruses and many different animal species and participate in a variety of cellular activities (*25, 26*). This domain, which consists of 85−90 residues including 3 highly conserved Trp/Tyr residues and a C-terminal basic region, binds to purine-rich DNA sequences containing the consensus 5′-GGAA/T-3′ (*25*−*27*). The crystal structure of the specific PU.1 ETS−DNA complex (*28*) shows a winged helix−turn−helix (HTH) motif in which the protein inserts helix α3 into the DNA major groove at the core 5′-GGA-3′ consensus where strictly

[†] This investigation was supported by an Ontario Graduate Scholarship and Merck Frosst Fellowship in Pharmacy to G.M.K.P. and by grants from the Natural Science and Engineering Research Council of Canada to R.B.M. Preliminary results of this work were presented at the Annual Meeting of the Biophysical Society, Boston, MA, on Feb 21, 2001.

* To whom correspondence should be addressed at the Department of Pharmaceutical Sciences, University of Toronto, 19 Russell St., Toronto, Ontario M5S 2S2, Canada. Phone: (416) 978-7332, Fax: (416) 978-8511, E-mail: rob.macgregor@utoronto.ca.

[‡] Present address: Marie Curie Research Institute, Limpsfield Chart, Oxted, Surrey RH8 0Tl, U.K.

[1] Abbreviations: BSA, bovine serum albumin; DBD, DNA-binding domain; Ig, immunoglobulin; IPTG, isopropyl β-D-thiogalactoside; PMSF, phenylmethylsulfonyl fluoride; SDS−PAGE, sodium dodecyl sulfate−polyacrylamide gel electrophoresis; TBE, 89 mM Tris base, 89 mM boric acid, 2 mM Na_2EDTA, pH 8.3; MOPS, 3′-(*N*-morpholino)propanesulfonic acid; HEPES, *N*-(2-hydroxyethyl)piperazine-*N*′-2-ethanesulfonic acid; CD, circular dichroism; DSO, direct search optimization; HTH helix−turn−helix; K_D, equilibrium dissociation constant; ΔC_p, change in heat capacity at constant pressure.

10.1021/bi015572q CCC: $22.00
Published on Web 01/22/2002

FIGURE 1: λB DNA probe used in this study (*36*−*38*). The cognate sequence (with the 5′-GGAA-3′ consensus shaded in gray) is flanked by a trinucleotide G·C track; the 5′-AAA-3′ overhang facilitates end-labeling by T4 PNK.

conserved arginine residues make base-specific contacts while the adjacent loops contact backbone atoms a half-helical turn on either side at the minor groove. This pattern is reproduced in other specific ETS−DNA complexes, namely, human Ets-1 (*29*), murine Ets-1 (*30*), fli-1 (*31*), GABPα/β (*32*), SAP-1 (*33*), and Elk-1 (*34*), but differs significantly from other known HTH proteins (*35*).

We report here a thermodynamic characterization of the sequence-specific association of the DNA-binding domain (DBD) of murine PU.1 to the central 23-bp region of the λB site of the murine Igλ2−4 enhancer (*36*−*38*). Electrophoretic mobility shift and filter-binding titrations of PU.1 DBD by λB sites demonstrate that the stability of the specific protein−DNA complex is, within experimental uncertainty, only weakly sensitive to temperature within the physiological range. It also exhibits a weak dependence on solvent pH from 6.7 to 9.0 in phosphate and Tris buffers at 25 °C. In addition, the CD spectrum of the PU.1 DBD−λB complex is highly similar to a sum of the spectra of the unbound protein and DNA across the entire temperature range in which binding was observed. Taken together, these observations suggest that the sequence-specific PU.1 DBD−λB association is not motivated by coupled folding. To our knowledge, this is the first report on the thermodynamics of sequence-specific binding by an ETS protein. Since structural studies have demonstrated a highly homologous structural paradigm in sequence-specific binding by different ETS proteins (*33*, *35*), our results may find applications in understanding the thermodynamics of general site recognition by this family of transcription factors.

EXPERIMENTAL PROCEDURES

Materials. [γ-^{32}P]ATP (6000 Ci mol^{-1}) and poly(dA-dT)·poly(dA-dT) were purchased from Amersham Pharmacia Biotech. Thrombin and DNase I came from Boehringer Mannheim, T4 PNK from MBI Fermentas, and BSA from Calbiochem. Oligonucleotides were synthesized by ACGT Corp., Toronto, Ontario, Canada. Sources of other chemicals and materials are as indicated below. All reagents are of analytical grade or better.

DNA Preparation. A 64-nt DNA hairpin containing the central 23-bp region of the λ_B site of the murine Igλ2−4 enhancer was used (Figure 1). Radiolabeled probe was prepared with [γ-^{32}P]ATP and T4 PNK, and eluted into binding buffer (described below) through a polyacrylamide size-exclusion column (Bio-Spin 6, Bio-Rad) which also removed unincorporated [γ-^{32}P]ATP. The DNA was re-annealed by heating to 95 °C for 5 min followed by gentle cooling over 2 h. Unlabeled probe was scanned and quantified at 25 °C on an Aviv 14DS spectrophotometer (Lakewood, NJ), assuming an OD of 1 = 50 μg mL^{-1} at 260 nm and a calculated molecular weight of 19 701.

Protein Expression and Purification. The cloning and purification of the murine PU.1 DBD (amino residues 154−266, equivalent to the human protein numbering 152−264) was largely as described (*39*). The construct cDNA was subcloned into a pET15b vector (Novagen, Madison, WI), which added an *N*-terminal $(His)_6$ tag followed by a thrombin cleavage site. Transformed *E. coli* (BL21DE3-pLysS) was cultured in LB medium, induced with 1 mM IPTG, and subsequently lysed with Triton X-100. Cell lysate was loaded onto an immobilized Co^{2+} affinity resin (Clontech, Palo Alto, CA) and washed twice with 20 mM imidazole, and the target construct was eluted in a 500 mM imidazole buffer. The $(His)_6$ tag was cleaved by incubation with thrombin at 4 °C overnight in a Tris buffer (50 mM, 500 mM NaCl, pH 7.6) and removed by passing through the Co^{2+} resin. SDS−PAGE of eluates sampled at various stages demonstrated single bands (by Coomassie blue staining) after affinity chromatography and thrombin proteolysis at the expected mobility. After purification, EDTA and PMSF were added to 1 mM each, and the protein was stored in small aliquots at −78 °C. BSA and glycerol were added to aliquots in active use (to 0.2 μg/μL and 50%, respectively) and kept at −20 °C or lower. Periodic assays by gel electrophoretic mobility shift (see below) indicated that under these storage conditions the protein retained >95% specific binding after 60 days.

Quantitative Gel Electrophoresis Mobility Shift. PU.1 DBD (0.2−0.4 μM) and radiolabeled DNA probe (0.85 nM) were mixed with graded concentrations of unlabeled DNA, 0.1 μg of BSA, and 1.7 μg of poly[d(AT)] in 6 μL of binding buffer (25 mM Na_2HPO_4, 1 mM H_4EDTA, 10% glycerol, NaCl at the required concentration). The mixture was incubated at the stated temperature (±1 °C) for at least 60 min. Incubations above ambient temperature were carried out in a GeneAmp 2400 PCR thermocycler (Perkin-Elmer, Norwalk, CT) in which the tubes were closed against a heated top (103 °C) to prevent evaporation without the use of mineral oil. After incubation, 5.5 μL of each sample was loaded onto a running 8% polyacrylamide gel in a MOPS running buffer (23 mM NaMOPS, 89 mM boric acid, 2.5 mM Na_2EDTA, pH 7.4 at 30 °C without adjustment) at 30 ± 1 °C and electrophoresed at 200 V for 25 min. The gel was vacuum-dried onto filter paper and scanned radiometrically using an Ambis 4000 detector (Scanalytics, Billerica, MA).

Gel scans were visualized using One-Dscan (version 1.33, Scanalytics). Lane traces were fitted to exponentially modified Guassian distributions (to account for tailing peaks) along a linear baseline using PeakFit (version 4, SPSS Inc., Chicago, IL). Based on a 1:1 stoichiometry (*28*), K_D and total PU.1 DBD concentration, $[P]_t$, were estimated by fitting the integrated intensities of the bound and unbound bands to eq 1 using Origin (version 6.0, Microcal, Northampton, MA):

$$[D]_t[P]_t - ([D]_t + [P]_t + K_D)[DP] + [DP]^2 = 0 \quad (1)$$

where $[D]_t$ is the total DNA concentration and the integrated intensities of the (radiolabeled) bound and unbound bands are taken to represent the distribution of total DNA in the bound and unbound states at each concentration.

Filter-Binding Experiments. PU.1 DBD (~10 nM) was mixed with radiolabeled DNA probe (diluted to a known concentration with unlabeled probe), 0.25 μg of BSA, and 15 μg of poly[d(AT)] in 50 μL of binding buffer consisting of 25 mM Na_2HPO_4, sodium cacodylate, or Tris base at the

pH as described in the text and tables, 1 mM H_4EDTA, NaCl as stated, and 10% glycerol. Mixed cellulose nitrate−acetate filters (Millipore type HA, 0.45 μm pore size) were equilibrated for several hours in binding buffer. For each sample, after incubation to equilibrium at the desired temperature, a fresh filter was mounted onto a vacuum filtration apparatus, washed with 1 mL of binding buffer which had been equilibrated to the incubation temperature, and immediately loaded with 45 μL of binding mixture followed by a second 1.0 mL wash with binding buffer. The filter was aspirated for another 1 min and counted in 5 mL of scintillant (CytoScint, ICN, Costa Mesa, CA). Background binding (i.e., in the absence of PU.1 DBD) was followed similarly. Total DNA concentrations were determined by counting 3 μL of each remaining sample and 3 μL of the radiolabeled DNA stock.

For each experiment, radioactivity measurements were converted to concentrations using the total counts of the 3-μL sample and stock aliquots. Background binding increased linearly with DNA concentration to a maximum of ~15% of the total signal at the highest concentration of probe used (~3 μM). The total DNA, $[D]_t$, and apparent, background-subtracted complex, $[DP]_{app}$, concentrations were fitted to eq 1 with the substitution:

$$[DP] = \frac{[DP]_{app}}{\epsilon} \qquad (2)$$

where ϵ is the filter retention efficiency. $[P]_t$ was independently determined by control gel mobility shift experiements, and this value was used in the estimation of ϵ (typically 30−40%) and K_D.

Circular Dichroism Spectroscopy. PU.1 DBD, λB site DNA, and PU.1 DBD−λB complex were separately dialyzed against excess volumes of the same preparation of binding buffer (25 mM Na_2HPO_4, pH 7.4, 1 mM H_4EDTA, 200 mM NaCl, 10% glycerol) overnight at 4 °C. CD spectra from 198 to 310 nm were scanned at 1.0 nm increments at constant temperatures (±0.1 °C) on an Aviv 62A DS CD spectrometer (Lakewood, NJ). PU.1 DBD (ϵ_{280} = 22 190 M^{-1} cm^{-1}) and DNA concentrations were determined from accompanying dynode voltage plots. Thermal-induced unfolding of the protein was conducted at 2.0 ± 0.1 °C intervals with an equilibration time of 60 s at each temperature.

RESULTS

Stability of the Sequence-Specific PU.1 DBD−λB Complex Displays an Unusual Temperature Dependence. We have performed equilibrium titration experiments for the sequence-specific binding of the ETS domain of PU.1 to the λB site of the Igλ2−4 enhancer as a function of temperature under different buffer conditions by electrophoretic mobility shift (Figure 2, Table 1) and filter-binding titrations (Table 2). In phosphate buffers containing 150 or 250 mM Na^+, both techniques showed the unexpected result that K_D was, within experimental uncertainty, independent of temperature from 0 °C to at least 25 °C, and began to increase at higher temperatures. In the electrophoretic mobility shift series, K_D appeared to reach a slight trough at 37 °C for both salt conditions (Table 1); this was not observed in the filter-binding series, in which K_D either remained constant or increased slightly up to this temperature (Table 2). The increase in K_D above 37 °C appeared linear in a van't Hoff representation of the data (Figure 3). In all, K_D varied a mere 10-fold across a temperature range of 52 °C with little variation in the physiologic range. No electrophoretic mobility shift was observed at 60 °C in 150 mM Na^+. The complex appeared to be somewhat more stable at 150 mM compared to 250 mM Na^+, but not beyond experimental error. Thus, the temperature dependence of K_D exhibited two qualitatively different régimes—a weakly temperature-dependent one from 0 °C to between 25 and 37 °C, and a temperature-dependent one above 37 °C (Figure 3).

We also investigated the pH dependence of PU.1 DBD−λB association by filter binding (Figure 4). In phosphate

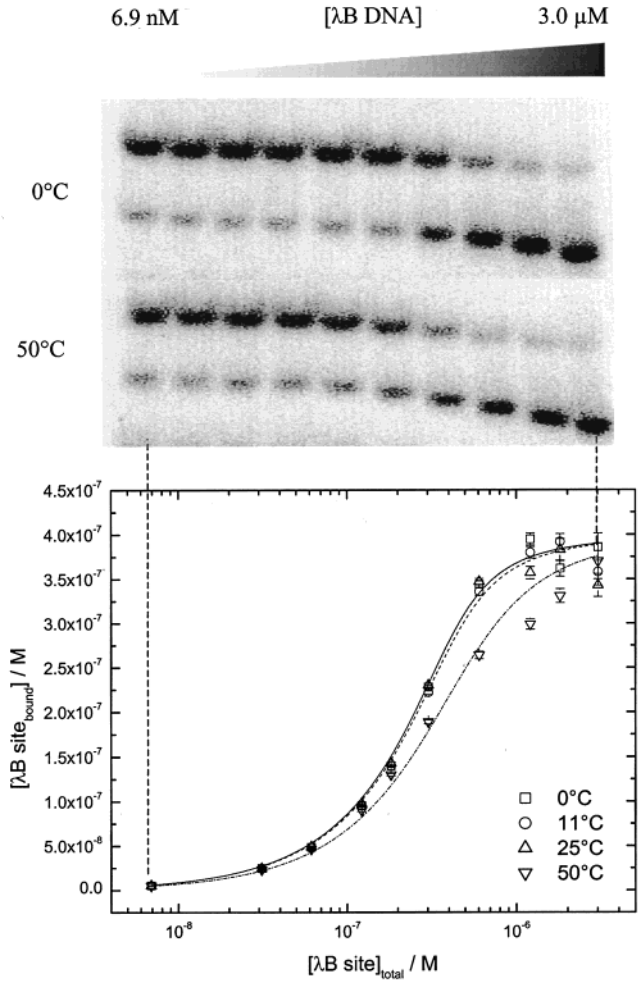

FIGURE 2: Representative electrophoretic gel mobility shift titration of the PU.1 DBD with λB site DNA. 0.4 μM PU.1 DBD in 25 mM Na_2HPO_4, 1 mM H_4EDTA, 200 mM NaCl, pH 7.4, was incubated at 25 °C to equilibrium with 0.1 μg of BSA, 1.7 μg of poly[d(AT)]·poly[d(AT)], and graded concentrations of the λB site (each sample containing the same amount of radiolabeled probe). Electrophoresis was carried out as described under Experimental Procedures. The data shown here are taken from a single experiment in which aliquots of the protein−DNA mixture were simultaneously incubated at the indicated temperatures and electrophoresed. The radiometric gel images for two temperatures (0 and 50 °C) are shown, aligned to show the effect of increasing λB DNA concentrations from left to right. As bound DNA accounted for a decreasing fraction of total λB DNA concentration, the intensity of the bound band decreased. The curves are best fits of the data to eq 1 with a common capacity parameter ($[P]_t$) assigned to the entire data set.

Table 1: Temperature Dependence of K_D for the Interaction between the PU.1 ETS Domain and the λB Site by Quantitative Electrophoretic Mobility Shift

$[Na^+]$/mM[a]	T/°C	pH	$K_D \times 10^{-8}$/M
150	0	7.4	3.5 ± 0.3
150	11	7.4	4.4 ± 0.4
150	25	7.4	4.3 ± 0.4
150	37	7.4	3.5 ± 0.4
150	50	7.4	9.8 ± 1.0
150	60	7.4	—[b]
250	0	7.4	5.0 ± 0.4
250	11	7.4	5.3 ± 0.6
250	18	7.4	5.0 ± 0.6
250	25	7.4	4.9 ± 0.4
250	37	7.4	3.2 ± 0.5
250	50	7.4	11 ± 1

[a] Buffer contained 25 mM Na_2HPO_4, 1 mM H_4EDTA, 10% glycerol, and 100 or 200 mM NaCl to give the stated total $[Na^+]$. Each sample (6 μL) also contained 0.1 μg of BSA and 1.7 μg of poly[d(AT)]. [b] Bound λB DNA was not observed.

Table 2: Temperature Dependence of K_D for PU.1 ETS−λB Association by Filter Binding

buffer	$[Na^+]$/mM[a]	T/°C	pH[b]	$K_D \times 10^{-8}$/M
25 mM Na_2HPO_4	250	25	6.7	5.1 ± 0.5
	250	0	7.4	4.1 ± 0.6
	250	12	7.4	4.3 ± 0.8
	250	25	7.4	4.0 ± 0.6
	250	37	7.4	9.1 ± 1.2
	250	45	7.4	20 ± 2
	250	52	7.4	39 ± 7
	250	25	8.1	4.5 ± 0.5
25 mM Na cacodylate	225	0	6.7	9.3 ± 1.2
	225	12	6.7	7.9 ± 2.3
	225	25	6.7	8.5 ± 1.1
	225	37	6.7	7.3 ± 1.8
25 mM Tris	250	0	9.0	5.9 ± 0.8
	250	12	8.7	6.7 ± 1.0
	250	25	8.3	7.8 ± 1.0
	250	37	8.0	9.0 ± 0.9
	250	45	7.8	25 ± 3
	250	52	7.6	43 ± 7
	250	25	9.0	6.3 ± 0.5

[a] Included contribution from buffer salt and added NaCl. Buffer also contained 1 mM H_4EDTA and 10% glycerol; each sample (50 μL) was co-incubated with 0.25 μg of BSA and 15 μg of poly[d(AT)] (previously dissolved in the stated buffer). [b] Buffers were prepared at 25 °C. The pH of Tris buffer at other temperatures was measured directly.

buffer at 25 °C, K_D did not change beyond experimental error with pH over a range of 6.7−8.1. The observed K_D at pH 9.0 at 25 °C in Tris buffer was somewhat higher, but remains in line with that observed in this buffer at the same pH at 0 °C (cf. Table 2 and Figure 3), so this difference from the phosphate buffer data appeared to be particular to Tris and not due to any coupled protonation equilibria. As in the case of temperature dependence, the variation in K_D spanned a range of only about 2×10^{-8} M from pH 6.7 to pH 9.0. The lack of a significant pH dependence was confirmed by parallel temperature dependences in phosphate buffer at pH 7.4, cacodylate buffer at pH 6.7, and Tris buffer at comparable Na^+ concentrations. Tris has a large positive enthalpy of ionization ($\Delta H_{ion} = 47.4$ kJ/mol; *40*), and the 25 mM Tris buffer used underwent a pH change of −1.4 units from 0 to 52 °C (Table 2), but the temperature dependence of K_D values in this buffer was nearly identical

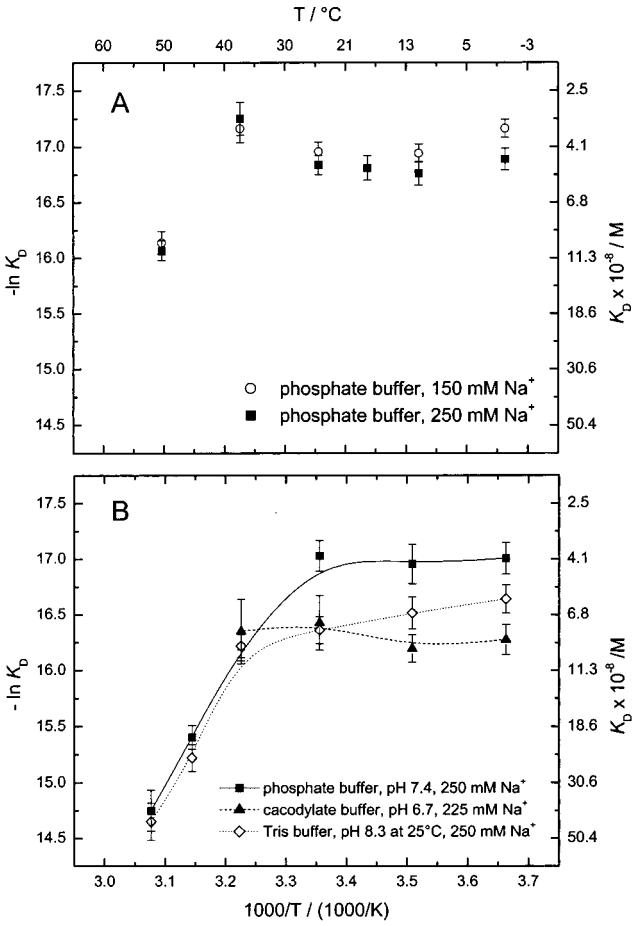

FIGURE 3: Energetics of the sequence-specific association of PU.1 DBD and λB DNA. Protein and DNA were incubated to equilibrium under different buffer conditions and separated by (A) gel mobility shift or (B) filter binding as described under Experimental Procedures. Numerical values and additional information are given in Tables 1 and 2. The lines in panel B are intended only to guide the eye.

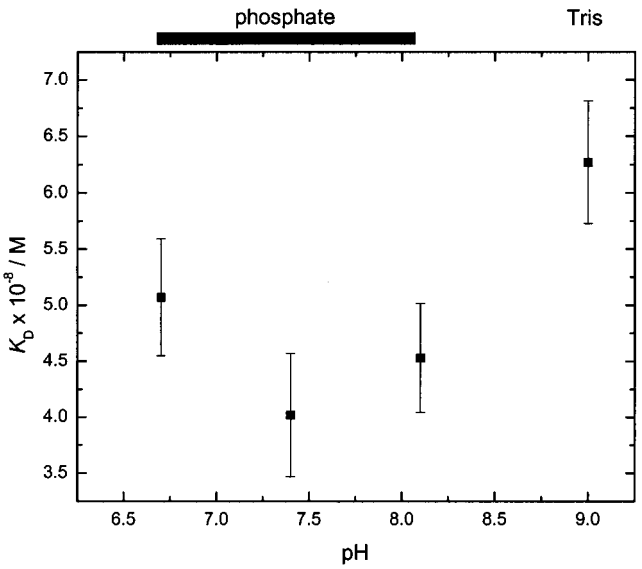

FIGURE 4: pH-dependence of the dissociation constant for the PU.1 DBD−λB complex at 25 °C in 250 mM Na^+ as determined by filter binding. Experiments at pH 6.7−8.1 were performed in 25 mM phosphate buffer and at pH 9.0 in Tris buffer (both containing 250 mM Na^+) as described in the text and Table 2, where the numerical values are given.

to that observed in phosphate buffer, which has a much smaller $\Delta H_{ion} = 5.12$ kJ/mol (*40*), and cacodylate buffer, which has a small negative $\Delta H_{ion} = -1.97$ kJ/mol (*40*).

UV/CD Spectroscopy. CD spectra of the unbound PU.1 DBD in phosphate-binding buffer (pH 7.4) were obtained from 198 to 310 nm at temperatures from 0 to 90 °C (Figure 5A). In the far-UV region, a CD signature with minima at 208 and 222 nm was observed. These minima were observed at temperatures up to 50 °C. Consistent with a macroscopically two-state transition, two isodichroic points are apparent, one at 230 nm and the minima at 208 nm is also isodichroic. This pattern is characteristic of α helices, and the large amplitude of the signal might have overwhelmed β sheet contributions (*28*). It was not possible to measure the CD signal below 198 nm due, in part, to strong absorption by the buffer, which was matched to the conditions of the binding experiments.

The ellipticity, θ, at 222 nm was followed as a function of temperature to study the melting behavior of the free protein (Figure 5B). Consistent with the presence of the two isodichroic points, the data was adequately described by a two-state, unimolecular transition model assuming a constant ΔC_p:

$$\Theta_{obs} = \frac{\Theta_N + m_N T + (\Theta_U + m_U T)\exp\left[\frac{\Delta H_m}{R}\left(\frac{1}{T_m} - \frac{1}{T}\right)\right]}{1 + \exp\left[\frac{\Delta H_m}{R}\left(\frac{1}{T_m} - \frac{1}{T}\right)\right]} \quad (3)$$

where the subscripts N and U refer to the native and unfolded states, respectively, m is the slope of the lower and upper baselines, R is the universal gas constant, and ΔH_m is the enthalpy of unfolding at the melting temperature T_m. The fit yielded $T_m = 54.5 \pm 0.6$ °C and $\Delta H_m = 180 \pm 17$ kJ/mol. Analogous data for the λB site under identical conditions were also determined by monitoring UV absorption at 260 nm, and we found $T_m = 77.2 \pm 0.1$ °C and $\Delta H_m = 142 \pm 3$ kJ/mol (data not shown). Thus, while the melting temperature of the λB DNA is above the temperature at which binding is abolished, thermal stability of the PU.1 DBD may impact on the observed K_D for site recognition.

As CD is highly sensitive to macromolecular conformation, we also wished to use this technique to detect conformational changes that might occur upon formation of the complex. To this end, we determined the extent to which the CD spectrum of the PU.1 DBD−λB complex could be expressed as a linear combination of the CD spectra of unbound PU.1 DBD and the λB site. On one hand, a noninteracting mixture would predict a perfect deconvolution (within experimental error) of the normalized spectrum of the mixture into the corresponding spectra of the components; on the other, a significant lack of agreement between could reveal a perturbation in the secondary structure of one or both of the components. A "noninteracting" fit was not expected as the components do interact, and the resultant new transition dipoles should alter to some degree the CD spectral behavior of the complex. Nonetheless, close agreement would be consistent with a "rigid-body" association by the protein and DNA.

A direct search optimization (DSO) approach (*41*) was employed to empirically deconvolve the observed CD spectra

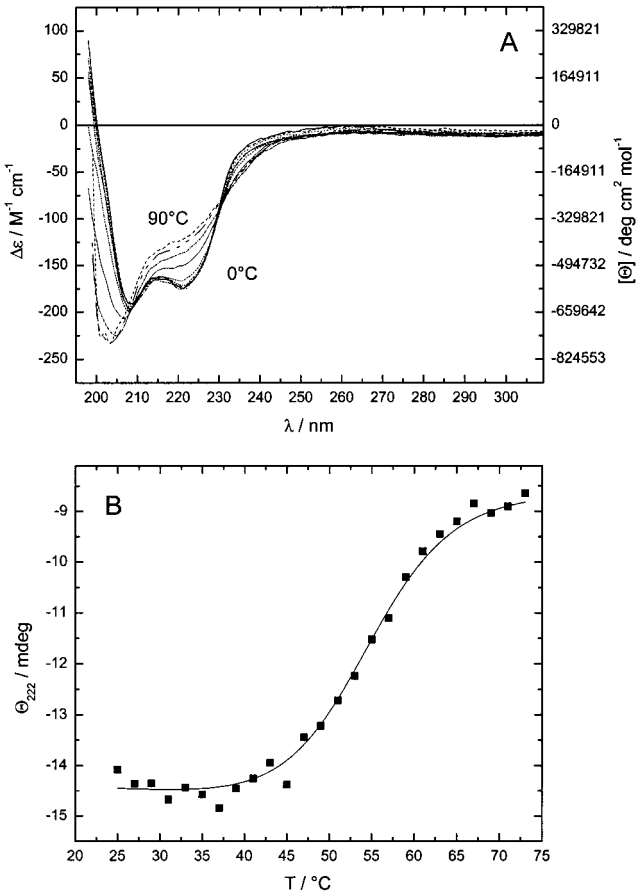

FIGURE 5: CD spectroscopic characterization of the PU.1 DBD. PU.1 DBD was extensively dialyzed in 25 mM Na_2HPO_4, 200 mM NaCl, 1 mM H_4EDTA, and 10% glycerol. (A) Buffer-subtracted spectra from 198 to 310 nm were scanned at 10.0 ± 0.1 °C intervals. (B) Thermal-induced denaturation was followed by the change in ellipticity at 222 nm at 2.0 ± 0.1 °C intervals with 2-min equilibration at each temperature. The line represents the best fit of the data to a two-state unimolecular transition, eq 3, yielding a van't Hoff enthalpy of unfolding $\Delta H_m = 180 \pm 17$ kJ/mol at $T_m = 54.5 \pm 0.6$ °C. $r^2 = 0.997$.

of the PU.1 DBD−λB complex at 10.0 ± 0.1 °C intervals from 0 to 60 °C in terms of the CD spectra of the unbound components at the corresponding temperatures. Solutions containing micromolar concentrations of the unbound components and the complex (with excess λB DNA to ensure stoichiometric binding of PU.1 DBD) were extensively dialyzed in the same binding buffer to avoid any variation with different preparations. The model used is a simple linear combination of the spectra of the unbound components:

$$CD_{complex}(\lambda) = f_{PU.1}CD_{PU.1}(\lambda) + f_{\lambda B}CD_{\lambda B}(\lambda) \quad (4)$$

where f_i is the scaling coefficient for each component $CD_i(\lambda)$. Since it was not possible to spectrometrically quantitate the concentrations of the free and bound DNA in the mixture solution, the raw, unnormalized ellipticities of the unbound components (at approximately the same concentrations as in the mixture) were used in the fitting as their amplitudes are of the same order of magnitude as the observed signal of the mixture. This would prevent potential numerical pitfalls arising from multiplying numbers of vastly different magnitudes as in the case if normalized ellipticities were used. The scaling coefficients would then be related to the

Table 3: Fitting Parameters for Deconvolution of the CD Spectrum of the PU.1 DBD−λB Complex

			R		
T/°C	$c_{PU.1}^{mix}/\mu M$[a]	$c_{\lambda B}^{mix}/\mu M$[b]	DSO[c]	gel[d]	r^2[e]
0	11.2	13.8	0.81	0.88 ± 0.20	0.989
10	10.8	13.8	0.78	nd[f]	0.991
20	10.3	13.7	0.75	0.88 ± 0.19	0.993
30	9.9	13.8	0.71	nd	0.993
40	9.1	13.8	0.65	nd	0.995
50	8.2	14.0	0.59	0.91 ± 0.18	0.996
60	7.4	13.9	0.53	nd	0.996

[a,b] Computed from eq 5, $c_{PU.1}^{alone} = 17.7\ \mu M$, $c_{\lambda B}^{alone} = 8.1\ \mu M$. [c] $R = c_{PU.1}^{mix}/c_{\lambda B}^{mix}$. [d] Determined as for gel mobility shift titration as described under Experimental Procedures. [e] DSO was adapted to minimize the sum of squares weighted to the inverse signal-to-noise ratio in the dynode voltage (the physically measured quantity) of the instrument at each wavelength scanned and r^2 = (regression SS)/(total SS). [f] Not determined.

"actual" concentrations in the mixture by

$$f_i = \frac{c_i^{mix}}{c_i^{alone}} \quad (5)$$

where the superscripts refer to the concentration of component *i* contributing to the observed signal in the PU.1 DBD/λB mixture or alone.

The distribution of the bound and unbound λB DNA at these temperatures was independently followed by electrophoretic mobility shifts of a small aliquot of the dialyzed mixture spiked with 37.5 fmol of radiolabeled λB DNA in a small volume (gels not shown). According to this technique, the bound-to-unbound ratio R^{gel} did not change significantly across the entire temperature range investigated, as expected given the saturating concentrations used relative to the K_D at these temperatures (cf. Tables 1 and 2).

The results of the DSO fits are shown in Figure 6 and Table 3. In each case, an excellent empirical fit could be made at each temperature studied ($r^2 > 0.98$). Much of the lack in fit occurred at wavelengths above 240 nm where the fit was higher than the observed spectra of the complex, and especially at the peak and shoulder above 270 nm; this disparity diminished with increasing temperature (Figure 6), resulting in a modest increase in the goodness-of-fit (Table 3). At the same time, $f_{PU.1}$ decreased at progressively larger steps with increasing temperature from a fitted $c_{PU.1}$mix value of 11.2 μM at 0 °C to 7.4 μM at 60 °C; this happened because most of the changes in the complex's spectra with increasing temperature occurred in the far-UV region, and this trend qualitatively correlated with the temperature-dependent variation in K_D (Figure 3; Tables 1 and 2). In contrast, $f_{\lambda B}$ remained remarkably constant, corresponding to a concentration of 14 μM for unbound λB DNA (Table 3), which closely matched the value calculated from the known amount of DNA used (5.6 nmol), assuming no loss into the dialysate from the 0.1 kDa cutoff dialysis membrane, and an approximate retentate volume of 400 μL. Thus, $f_{PU.1}$ was changed in each case to accommodate the fit. As an actual change in total PU.1 DBD concentration is not physically meaningful, this occurrence ought to be interpreted as a change in the CD contribution of the PU.1 DBD. We note that the melting temperature of the PU.1 DBD is only 55 °C and the independently determined R^{gel} estimates a temperature-invariant stoichiometric concentration PU.1 DBD that was most closely matched by $c_{PU.1}^{mix}$ at 0 °C (Table 3). These observations thus suggest that the protein undergoes a small progressive loss of secondary structure with increasing temperature, which is deleterious but evidently not fatal to complex formation.

DISCUSSION

Experimental Procedures. We have investigated the temperature- and pH-dependence of the association of the PU.1 DBD to the central 23-bp region of the λB site of the murine Igλ2−4 enhancer by gel electrophoretic mobility shift and filter-binding titrations. Gel mobility shift is a standard technique in thermodynamic and kinetic studies of noncovalent association by DNA-binding proteins, e.g., CAP (*42*, *43*), *Gal* repressor (*44*), *trp* repressor (*45*), as is filter binding, e.g., RNA polymerase holoenzyme (*20*), *cI* repressor (*46*), c-Myb DBD (*8*).

Nondenaturing gel electrophoresis allows separation of tightly bound protein-bound and free DNA despite a run time (25 min in our case) that is clearly much longer than the complex's solution half-life (*47*, *48*). Thus, even for complexes of moderate stability ($K_D = 10^{-9}-10^{-8}$ M; *48*), such as those of ETS proteins, this technique yields valid measurements of K_D (*27*). Arrowsmith and co-workers have used gel mobility shift (performed with much longer runtimes than the 25 min used here) to perform quantitative titrations on this protein−DNA system (*27*, *39*). We had also performed a number of preliminary experiments to probe possible effects of electrophoretic conditions on observed equilibrium constants. Neither the choice of running buffer (TBE, MOPS, or HEPES with or without boric acid at pH 7.4), its concentration, polyacrylamide content (from 6 to 14%), nor the duration of the run (up to 90 min) produced, within experimental error, differences in the determination of K_D (data not shown). The temperature of electrophoresis, however, did appear to have a mild influence on the observed K_D (for identically prepared samples incubated under the same temperature), producing an "enthalpy of electrophoresis" of approximately 4 kJ/mol (data not shown). To avoid possible complications, electrophoretic runs were conducted at a fixed temperature, and the running buffer was formulated to have a pH of 7.4 at that temperature. The quantitative consistency between these data and those from the filter-binding measurements (Tables 1 and 2) makes it highly unlikely that our thermodynamic observations were an artifact of the electrophoresis procedure but reflect the solution distribution of free and bound DNA at the time of loading, and also bolsters confidence that the observed thermodynamics of PU.1 DBD−λB site association is an intrinsic phenomenon of this biochemical system.

As we have studied the thermodynamics of PU.1 DBD−λB site association by measuring equilibrium binding, we were mindful of any indication that our van't Hoff assumptions might be invalid. Although the observed equilibrium was well described by a simple bimolecular reaction, it was possible that constituent processes might mutually compensate each other and yield anomalous thermodynamic parameters. If this were true, these compensatory contributions might be expected to vary differentially with solvent condi-

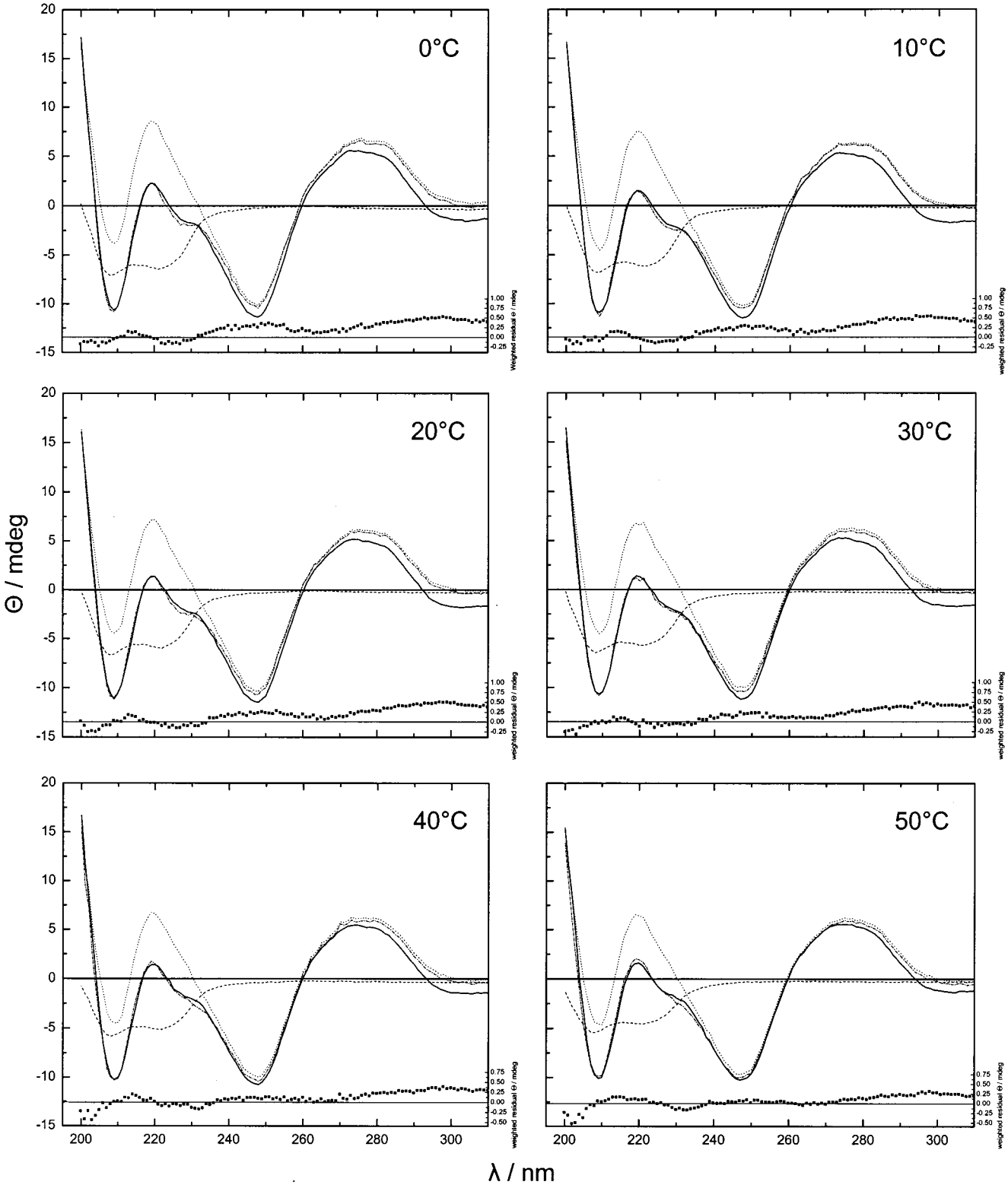

FIGURE 6: Deconvolution of the CD spectra of the PU.1 DBD−λB complex in terms of contributions from the unbound components. PU.1 DBD, λB DNA, and complex were dialyzed extensively against the same batch of buffer, and CD spectra were obtained from 200 to 310 nm at 10.0 ± 0.1 °C intervals. The raw spectra of unbound PU.1 DBD (dashed line) and λB DNA (dotted line) were fitted (dash−dotted line) nonparametrically to the observed PU.1 DBD−λB complex (heavy solid line) according to eqs 4 and 5 by direct search optimization. The weighted residual for each fit is shown at the bottom of each plot. Numerical values of the fitted parameters and global statistical details are given in Table 3. The spectra and fits for 60 °C are not shown.

tions, revealing unexpected values of ΔH, ΔS, and ΔC_p. However, in our experiments we examined a number of different salt and pH conditions (with buffers featuring widely different heats of ionization), and the temperature dependence of K_D remained the same under each of these conditions. Moreover, dissociation kinetics exhibited monoexponential decay consistent with simple, unimolecular dissociation of the complex (data not shown). Thus, there is no evidence to suggest that the assumptions inherent in the van't Hoff analysis (i.e., a macroscopically bimolecular

association) are invalid, and therefore the observed thermodynamic parameters appear to be intrinsic to the overall association mechanism.

The Energetic Profile of Sequence-Specific Binding of the PU.1 DBD Exhibits Striking Differences from Many Other Reported Systems. In many site-specific protein−DNA interactions reported in the literature, such as *Eco*RI (*13*, *18*), *lac* repressor (*13*), *E. coli trp* repressor (*9*), the Oct-1 transcription factor (*2*), and the TATA-binding protein from the hyperthermophilic archeon *P. woesei* (*6*), ΔH and $T\Delta S$ terms make large and comparable contributions to the observed ΔG. Moreover, these contributions exhibit a marked dependence on temperature over even a modest range (typically from 0 to 40 °C) indicative of a large negative ΔC_p which is usually taken as a constant. While many physical processes may contribute to ΔC_p (*14*, *15*), large values are generally interpreted as arising from changes in the hydration of the solvent-accessible surface area (SASA) upon binding, and are quantitatively modeled by a simple parametrization of the observed ΔC_p into changes in hydrophobic and polar SASA (*17*, *56*). The hydrophobic model predicts a global temperature minimum in K_D at a characteristic temperature in the physiological range at which $\Delta H = 0$, T_H, and an analogous minimum in ΔG_{obs} at T_S at which $\Delta S(T_S) = 0$ (*9*, *13*). In contrast to this "typical" energetic profile for sequence-specific protein−DNA interactions, we observed a remarkable insensitivity of the stability of the specific PU.1 DBD−DNA complex to temperature up to about 37 °C. Above this temperature, $-\ln K_D$ assumed an apparently linear descent with the inverse temperature (Figure 3). The hydrophobic model was able to formally fit the van't Hoff data in phosphate buffer, pH 7.4, as determined by filter binding, to yield a fitted $\Delta C_p = -2.5 \pm 0.4$ kJ mol^{-1} K^{-1}, $T_S = 28.6 \pm 1.2$ °C, and $T_H = 11.8 \pm 2.1$ °C, although the experimental $-\ln K_D$ does not show a distinct temperature maximum near the presumed T_H (Figure 7). This fitted value of ΔC_p is significantly smaller in magnitude than those reported for other sequence-specific protein−DNA systems, which are at least 5 kJ mol^{-1} K^{-1} (*9*) and typically much higher (*13*, *17*). Since the temperature-dependent curvature in K_D is dependent on not only ΔC_p but also T_H and T_S, it might be argued that this small magnitude of ΔC_p is "compensated" by a relatively small value of T_H. We note, however, that the value of T_H is in itself unusual for the majority of protein−DNA interactions reported, which is typically above 20 °C (*13*, *17*). We interpret this particular set of parameters to merely reflect the fact that the observed K_D for the PU.1 DBD−λB association, per se, lacks a distinct temperature minimum and is overall a modest function of temperature compared to other sequence-specific systems, varying a mere 10-fold across over a 50 °C change in temperature (Figure 3).

To the extent that the hydrophobic effect (and, specifically, a large observed negative ΔC_p) applied to sequence-specific protein−DNA interactions is primarily attributed to coupled folding in the protein (*17*, *18*), our CD spectroscopic results are consistent with this interpretation. Across the entire temperature range in which binding is observed, the CD spectra of the complex can be closely approximated by a linear combination of the spectra of the unbound components (Table 3). This observation is not altogether unexpected, for CD titration experiments with other systems with large

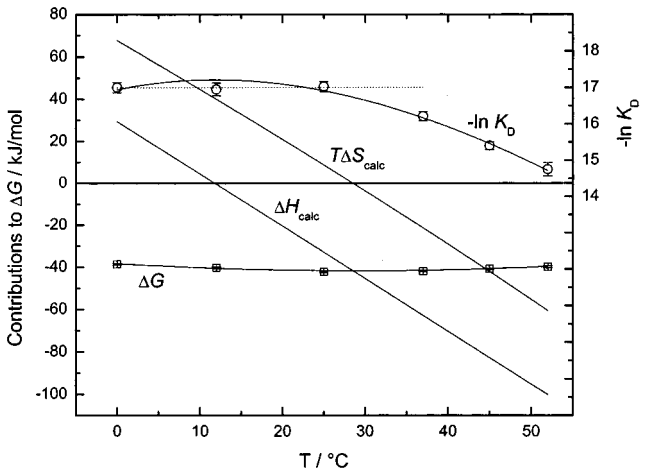

FIGURE 7: Thermodynamics of PU.1 DBD−λB site interaction in phosphate buffer containing 250 mM Na^+ at pH 7.4 according to the hydrophobic effect (*13*). The 3-parameter relationship $-\ln K_D = (\Delta C_p/R)[T_H/T - \ln(T_S/T) - 1]$ was used to fit the experimental filter binding data (circles) in phosphate buffer, pH 7.4. This yielded $\Delta C_p = -2.5 \pm 0.4$ kJ mol^{-1} K^{-1}, $T_H = 11.8 \pm 0.2$ °C, and $T_S = 28.6 \pm 1.2$ °C, where the subscripted T's represent the temperatures at which the ΔH_{calc} and ΔS_{calc} are zero, respectively. The observed free energy of association ΔG_{obs}, $\Delta H_{calc} = \Delta C_p(T - T_H)$, $\Delta S_{calc} = \Delta C_p \ln(T/T_S)$, and $\Delta G_{calc} = \Delta H_{calc} - T\Delta S_{calc}$ are also shown. The dotted line is a constant line fitted to the data from 0 to 25 °C, the fitted $-\ln K_D = 17.00 \pm 0.02$.

negative values of ΔC_p show significant spectral changes in the protein−DNA complex (*4*, *9*). We emphasize that a perfect fit is not, and indeed should not be, expected because the new interactions that occur as a result of association should perturb the CD signature of the complex. Some changes in the spectra of the complex were observed, namely, the hypodichroism in the complex's spectra above 240 nm, which diminished with increasing temperature as the observed K_D also began to rise noticeably above 37 °C (Figure 6). Taken together, the lack of distinctive changes in the CD spectrum of the PU.1 DBD−λB complex and the small fitted value of ΔC_p suggest that coupled folding is a minor or negligible contributor to the stability of the complex. The decline in the apparent value of $c_{PU.1}^{mix}$ and the modest improvement in the goodness-of-fit with increasing temperature (Table 3) may reflect the protein's thermal stability. Indeed, given that the melting temperature of the PU.1 DBD is only 55 °C, the binding energy may be utilized to stabilize the protein against denaturation, resulting in the observed rise in K_D above 37 °C. Quantitative confirmation of protein stabilization, however, is difficult with the present titration data, given the necessary assumptions regarding the thermodynamics of the "intrinsic" association equilibrium and the substantial parametrization required by such a scheme relative to the limited degrees of freedom in the data.

The notion that coupled folding is not a significant energetic contributor to PU.1 DBD site recognition is also supported by structural data. A solution NMR study of a 93-residue construct of the PU.1 ETS domain (*49*) showed that the secondary and tertiary structures in the protein observed in the crystal structure of the complex (*28*) were present in the free state. In particular, each of the native structural elements observed in the crystal structure was entirely present in the unbound solution NMR structure except for six residues at the C-terminal of helices α2 and

Table 4: Solvent-Accessible Surface Area and ΔC_p Calculation from the Crystal Structure of the PU.1 DBD−λB Complex (*28*)

	SASA/Å^2 [a]				
	PU.1 DBD[b]	DNA[b]	complex	ΔSASA	ΔC_p[e] (kJ mol^{-1} K^{-1})
Lee and Richards[c] (*51*)					
hydrophobic	2950.3	1718.1	3800.1	−879.9	−1.2 ± 0.1
polar	2783.4	4654.7	5957.2	−1480.8	0.9 ± 0.2
total	5733.7	6372.7	9745.7	−2360.7	−0.3 ± 0.3
Fraczkiewicz and Braun[d] (*52*)					
hydrophobic	2852.3	3418.9	5151.1	−1120.0	−1.5 ± 0.2
polar	3131.0	2232.8	4379.1	−984.7	0.6 ± 0.2
total	5983.2	5651.7	9530.2	−2104.7	−0.9 ± 0.3

[a] Values are the mean of the two observed complexes in the asymmetric unit. (PDB ID: 1pue, *28*). [b] Computed in the absence of the other binding component. [c] Using ACCESS version date March 6, 1983, with a water probe radius of 1.4 Å and a Z-step of 0.25 Å. Decreasing the Z-step to 0.08 Å produced negligible changes to the results. [d] Using GETAREA 1.1 at http://www.scsb.utmb.edu/cgi-bin/get_a_form.tcl with a water probe radius of 1.4 Å. The differences between the two models stem largely from the assignment of polar and hydrophobic groups based on atom identity (*51*) or functional groups (*52*). [e] Parametrization proposed by Spolar and Record (*17*): ΔC_p/(J mol^{-1} K^{-1}) = (1.3 ± 0.2)ΔSASA$_{hydrophobic}$/Å + (−0.6 ± 0.2)ΔSASA$_{polar}$/Å.

α3. It is clear that the coil-to-helix transition of these six residues did not make a significant incremental contribution to the overall helical content of the PU.1 DBD−λB complex, as judged by the DSO fits of the CD data (Figure 6, Table 3). The authors also reported that the 12-residue loop between α2 and α3 was unusually flexible in the unbound PU.1 DBD and proposed that it helped the docking of the recognition helix α3 into the DNA major groove at 5′-GGAA-3′. While it is not possible to evaluate this proposal on binding specificity directly with our present results, it is reasonable to expect that reduction of conformational entropy in the absence of folding would not contribute strongly to the observed ΔC_p.

With these considerations in mind, and noting that in the crystal structure the PU.1 DBD covers a relatively long stretch of DNA, we took the crystal structure of the nucleoprotein (Protein DataBank ID: 1pue, *28*) and calculated the changes in SASA from simple juxtaposition of the two components in order to estimate the contribution due to dehydration of the binding surfaces to ΔC_p using the parametrization proposed by Spolar and Record (*17*). The changes in hydrophobic and polar SASA calculated according to the methodology of Lee and Richards (*50*) or Fraczkiewicz and Braun (*51*) yielded estimates of ΔC_p (due to hydration changes) that are small, at best about half the magnitude of the formal value of $\Delta C_p = -(2.5 \pm 0.4)$ kJ mol^{-1} K^{-1} obtained by fitting the observed K_D to the hydrophobic model (Table 4). Although the total base sequence of the DNA used in the crystal structure is somewhat different and shorter (16 bp), DNase I and hydroxyl radical footprinting experiments have confirmed a highly homologous DNA footprint in specific PU.1 ETS complexes with different cognate sequences, including the crystal structure sequence and the λB site used in our experiments (*35*, *37*, *38*). We also note that in the crystal structure, protein−DNA contacts are observed only along a 11-bp tract centered about the 5′-GGAA-3′ consensus even though the complete sequence is 5 bp longer (*28*, *35*). This 11-bp tract is identical to the λB site except for the two bases immediately 5′ to the consensus 5′-GGAA-3′ (5′-AA-3′ in the λB site instead of 5′-GG′-3′). Thus, the structurally derived ΔSASA estimates should be applicable, within the error inherent in this method, to the PU.1 DBD−λB complex as well. The remaining "excess" $\Delta C_p \sim -1$ kJ mol^{-1} K^{-1} is small and can be accounted for by contributors such as entropic penalties due to binding, changes in vibrational modes (*14*), and electrostatic interactions (*15*) which are operative. Here again we see no need to invoke the hydrophobic effect as a significant player.

Our titration data across a pH range from 6.7 to 9.0 indicated that the observed K_D was weakly dependent on pH. The observed K_D was marginally higher at pH 9.0 in Tris buffer; this might be suspected as this pH is near the pK_a of the N-terminus of the protein, but a connection to significant proton uptake or release is unlikely, because the K_D values in Tris buffer at the same pH at 0 and 25 °C were equal within experimental error. If proton linkage were important to the energetics of association, significant differences in the temperature dependence of the observed K_D would be expected among the different buffers, especially given the large heat of ionization of Tris. However, we observed a remarkable similarity in the temperature profile of the observed K_D in all the buffers investigated. A basis for this lack of pH dependence may be understood from the crystal structure (*28*) in which the N-terminus is solvent-exposed and situated away from the DNA contact interface. The PU.1 DBD construct used in our experiments also contained a short N-terminal remnant of the cleaved $(His)_6$ tag from purification, which was expected to be conformationally unrestricted in solution.

Although extensive comparative studies have been performed to explore differences among sequence-specific complexes formed by ETS proteins (*27*, *33*−*35*, *52*), the thermodynamics of site recognition by ETS proteins remain inadequately explained by the detailed structural knowledge of this family of transcription factors. Our findings have discounted coupled folding and coupled proton uptake or release as major energetic contributors to sequence-specific binding. It is also evident that the enthalpy change arising from binding is not the principal component of the association free energy in the physiological temperature range. Using uncharged methylphosphonate bases, Soukup and Maher (*53*) demonstrated that the energetic cost of the overall 8° bend observed in the DNA in the PU.1 nucleoprotein complex could be compensated by the neutralization of backbone phosphates on one face of the DNA helix. The importance of charge neutralization to the binding energetics would lead to the prediction of a large salt dependence in the observed K_D. Binding experiments with [Na^+] from 150 to 250 mM produced only an insignificant increase in K_D (Table 1, Figure

3). Since the polyelectrolyte theory predicts a linear increase in ln K_D with ln [Na^+] (δ ln K_D/δ [Na^+] = $Z\psi$, where Z is the number of Na^+ released and $\psi = 0.88$ for dsDNA for [Na^+] $\leq$ 0.5 M; *54, 55*), this lack of salt-dependence in K_D across a range of 100 mM would impose at best a modest upper limit for the significance of counterion release as an energetic contributor to PU.1 DBD−λB association. A mitigating factor in evaluating the energetic role of charge neutralization is the tendency of the protein to polymerize under "low"-salt conditions, which rendered it difficult to maintain unaggregated samples at concentrations above about 30 μM at 250 mM Na^+ even in the presence of cognate DNA in the solution (data not shown; see also a discussion of the same problem by Jia et al., *50*). This complication could limit the applicability of a linear salt-dependence over a wide range of salt concentration. At the least, however, it appears that phosphate neutralization does not drive DNA binding in the physiologically relevant salt range tested in our experiments (150−250 mM), in contrast to other specific systems, for instance, *Lac* repressor−O^{sym} interactions (*56*).

Quantitative applications of the hydrophobic effect find their greatest usefulness in systems for which the magnitude of the observed ΔC_p is large (*15*). In the present case, it is reasonable to consider the van't Hoff data, which estimate an "anomalously" small value of ΔC_p and are generally a weak function of temperature, out of the context of this oft-cited model. Without being unnecessarily speculative, one can adopt the phenomenological view that the apparent insensitivity of K_D to temperature from 0 to 25 °C (Figure 7, dotted line) indicates a negligible ΔH_{obs} and ΔC_p *for that temperature range*. Thus, to a first approximation, the association is driven entirely by entropy, i.e., $\Delta G_{obs} \approx -T\Delta S_{obs}$. The emergent sensitivity to heat above 25 °C is seen as ΔH_{obs} shifts to a more negative value; the data from 37 to 52 °C interpolate to a constant value of $\Delta H_{obs} = -82 \pm 1$ kJ/mol. (Figure 3). This interpretation implies an attendant (small) negative ΔC_p that is itself a weak function of temperature (at least in the range investigated). A temperature-dependent ΔC_p may be intrinsic and/or the net effect of multiple opposing, macroscopically apparent processes coupled to the overall association. We plan to test the validity of this alternative hypothesis by observing the temperature sensitivity of the association equilibrium to conditions that probe the effects of entropic contributors. For example, the movement of ions and water molecules between macromolecular surfaces and the bulk solution is sensitive to pressure (*57*), and a significant transition volume may attend the application of hydrostatic pressure (*58*). Similarly, one can employ osmotic pressure (*23, 24, 59*) to probe the role of differential hydration in modulating the equilibrium.

In a broader perspective, our current uncertainty in explaining the thermodynamics of site recognition by ETS domains bears on the current paradigm of the specificity of protein−DNA interactions. On one hand, specific binding is the net result of an interplay among base-specific interactions, the polyelectrolyte effect (*57*), the hydrophobic effect, and entropic penalties of bimolecular association. Despite this apparent complexity, hydrophobic effects due to coupled folding are thought to dominate the energetics of site-specific protein−DNA binding (*17, 18*). On the other hand, studies of nonspecific DNA binding by model oligopeptides (*21, 22*) identify entropic, and in particular electrostatic, factors as the primary energetic contributors to nonspecific association (*18*), although significantly enthalpic processes such as protonation equilibria (*60*) and specific ion release (*61*) may be coupled. While a number of systems have been observed to conform to this description, there are also exceptions. For example, Koblan and Ackers (*62*) obtained linear van't Hoff plots for the site-specific interactions of the λ cI repressor at the O_R sites indicating a mainly entropically driven association. For MM17, a covalently linked dimer of the transcription factor MASH-1, strikingly similar temperature dependence of the observed ΔH and ΔS is observed for both specific and nonspecific DNA binding ($\Delta C_p \sim -2$ kJ mol^{-1} K^{-1} for both; *3*). Our studies with the ETS domain of PU.1 are also apparently incongruent, where the energetic profile we observed for the sequence-*specific* binding of the PU.1 DBD is similar to that observed for the binding of Cro (*12*), also a HTH protein, to *nonspecific* DNA at corresponding temperatures. In nonspecific Cro−DNA interactions, $-T\Delta S_{obs}$ is the greater contributor to the ΔG_{obs} while ΔH is temperature-invariant between 4 and 20 °C (above which thermal denaturation of the protein begins to contribute to the ΔH_{obs}). Further thermodynamic characterizations on ETS−DNA interactions and data on many more protein−DNA systems may confirm the suspicion that, perhaps not surprisingly, nature exploits multiple strategies in achieving binding specificity.

ACKNOWLEDGMENT

We are grateful to Dr. Cheryl H. Arrowsmith of the Department of Medical Biophysics, University of Toronto, for providing the plasmid for the PU.1 DBD and access to facilities for the expression and purification of the protein. Mr. Blair R. Szymczyna's assistance with the expression and purification procedure is greatly appreciated. We also thank Dr. Tigran V. Chalikian of the Department of Pharmaceutical Sciences for use of the Aviv CD spectrometer, Mr. David N. Dubins for implementating the DSO routines, and Dr. Ekaterina Protozanova for fruitful ideas and discussions.

REFERENCES

1. Lipps, G., Stegert, M., and Krauss, G. (2001) *Nucleic Acids Res. 29*, 904−913.
2. Lundbäck, T., Chang, J.-F., Phillips, K., Luisi, B., and Ladbury, J. E. (2000) *Biochemistry 39*, 7570−7579.
3. Sieber, M., and Allemann, R. K. (2000) *Nucleic Acids Res. 28*, 2122−2127.
4. Privalov, P. L., Jelesarov, I., Read, C. M., Dragan, A. I., and Crane-Robinson, C. (1999) *J. Mol. Biol. 294*, 997−1013.
5. Lunbäck, T., Hansson, H., Knapp, S., Ladenstein, R., and Härd, T. (1998) *J. Mol. Biol. 276*, 775−786.
6. O'Brien, R., DeDecker, B., Fleming, K. G., Sigler, P. B., and Ladbury, J. E. (1998) *J. Mol. Biol. 279*, 117−125.
7. Zou, Y., Bassett, H., Walker, R., Bishop, A., Amin, S., Geacintov, N. E., and Van Houten, B. (1998) *J. Mol. Biol. 281*, 107−119.
8. Oda, M., Furukawa, K., Ogata, K., Sarai, A., and Nakamura, H. (1998) *J. Mol. Biol. 276*, 571−590.
9. Künne, A. G. E., Sieber, M., Meierhans, D., and Allemann, R. K. (1998) *Biochemistry 37*, 4217−4223.
10. Jin, L., Yang, J., and Carey, J. (1993) *Biochemistry 32*, 7302−7309.
11. Ladbury, J. E., Wright, J. G., Sturtevant, J. M., and Sigler, P. B. (1994) *J. Mol. Biol. 238*, 669−681.
12. Takeda, Y., Ross, P. D., and Mudd, C. P. (1992) *Proc. Natl. Acad. Sci. U.S.A. 89*, 8180−8184.

13. Ha, J.-H., Spolar, R. S., and Record, M. T., Jr. (1989) *J. Mol. Biol. 209*, 801−816.
14. Sturtevant, J. M. (1977) *Proc. Natl. Acad. Sci. U.S.A. 74*, 2236−2240.
15. Gallagher, K., and Sharp, K. (1998) *Biophys. J. 75*, 769−776.
16. Baldwin, R. L. (1986) *Proc. Natl. Acad. Sci. U.S.A. 83*, 8069−8072.
17. Spolar, R. S., and Record, M. T., Jr. (1994) *Science 263*, 777−784.
18. Jen-Jacobson, L. (1997) *Biopolymers 44*, 153−180.
19. Privalov, P. L. (1979) *Adv. Protein Chem. 33*, 167−241.
20. Strauss, H. S., Burgess, R. R., and Record, M. T., Jr. (1980) *Biochemistry 19*, 3496−3504.
21. Padmanabhan, S., Zhang, W., Capp, M. W., Anderson, C. F., and Record, M. T., Jr. (1997) *Biochemistry 36*, 5193−5206.
22. Zhang, W., Bond, J. P., Anderson, C. F., Lohman, T. M., and Records, M. T., Jr. (1996) *Proc. Natl. Acad. Sci. U.S.A. 93*, 2511−2516.
23. Sidorova, N. Y., and Rau, D. C. (1996) *Proc. Natl. Acad. Sci. U.S.A. 93*, 12272−12277.
24. Sidorova, N. Y., and Rau, D. C. (2000) *Biopolymers 53*, 363−368.
25. Sharrocks, A. D., Brown, A. L., Ling, Y., and Yates, P. R. (1997) *Int. J. Biochem. Cell. Biol. 29*, 1371−1387.
26. Wasylyk, B., Hahn, S. L., and Giovane, A. (1993) *Eur. J. Biochem. 211*, 7−18.
27. Szymczyna, B. R., and Arrowsmith, C. H. (2000) *J. Biol. Chem. 275*, 28363−28370.
28. Kodandapani, R., Pio, F., Ni, C.-Z., Piccialli, G., Klemsz, M., Mckercher, S., Maki, R. A., and Ely, K. R. (1996) *Nature 380*, 456−460.
29. Werner, M. H., Clore, G. M., Fisher, C. L., Fisher, R. J., Trinh, L., Shiloach, J., and Gronenborn, A. M. (1995) *Cell 83*, 761−771; erratum (1996) *Cell 87*, 2.
30. Donaldson, L. W., Petersen, J. M., Graves, B. J., and McIntosh L. P. (1996) *EMBO J. 15*, 125−134.
31. Liang, H., Mao, X., Olejniczak, E. T., Nettesheim, D. G., Yu, L., Meadows, R. P., Thompson, G., and Fesik, S. W. (1994) *Nat. Struct. Biol. 1*, 871−876.
32. Batchelor, A. H., Piper, D. E., de la Brousse, F. C., McKnight, S. L., and Wolberger, C. (1998) *Science 279*, 1037−1041.
33. Mo, Y., Vaessen, B., Johnston, K., and Marmorstein, R. (1998) *Mol. Cells 2*, 201−212.
34. Mo, Y., Vaessen, B., Johnston, K., and Marmorstein, R. (2000) *Nat. Struct. Biol. 7*, 292−297.
35. Pió, F., Kodandapani, R., Ni, C.-Z., Shepard, W., Klemsz, M., McKercher, S. R., Maki, R. A., and Ely, K. R. (1996) *J. Biol. Chem. 271*, 23329−23337.
36. Eisenbeis, C. F., Singh, H., and Storb, U. (1995) *Mol. Cell. Biol. 13*, 6452−6461.
37. Gross, P., Arrowsmith, A. H., and Macgregor, R. B., Jr. (1998) *Biochemistry 37*, 5129−5135.
38. Gross, P., Yee, A. A., Arrowsmith, A. H., and Macgregor, R. B., Jr. (1998) *Biochemistry 37*, 9802−9811.
39. Yee, A. A., Yin, P., Siderovski, D. P., Mak, T. W., Litchfield, D. W., and Arrowsmith C. H. (1998) *J. Mol. Biol. 279*, 1075−1083.
40. Kozlov, A. G., and Lohman, T. M. (2000) *Proteins: Struct., Funct., Genet. 4*, 8−22.
41. Luus, R., and Jaakola, T. H. I. (1973) *AIChE. J. 19*, 760−766.
42. Fried, M. G., and Daugherty, M. A. (1998) *Electrophoresis 19*, 1247−1253.
43. Fried, M. G., and Liu, G. (1994) *Nucleic Acids Res. 22*, 5054−5059.
44. Brenowitz, M., Jamison, E., Majumadar, A., and Adhya, S. (1990) *Biochemistry 29*, 3374−3383.
45. Carey, J. (1988) *Proc. Natl. Acad. Sci. U.S.A. 85*, 975−979.
46. Senear, D. F., and Batey, R. (1991) *Biochemistry 30*, 6677−6688.
47. Cann, J. R. (1989) *J. Biol. Chem. 29*, 17032−17040.
48. Cann, J. R. (1996) *Anal. Biochem. 237*, 1−16.
49. Jia, X., Lee, L. K., Light, J., Palmer, A. G., and Assa-Munt, N. (1999) *J. Mol. Biol. 292*, 1083−1093.
50. Lee, B., and Richards, F. M. (1971) *J. Mol. Biol. 55*, 379−400.
51. Fraczkiewicz, R., and Braun, W. (1998) *J. Comput. Chem. 19*, 319.
52. Pió, F., Assa-Munt, N., Yguerabide, J., and Maki, R. A. (1999) *Protein Sci. 8*, 2098−2109.
53. Strauss-Soukup, J. K., and Maher, L. J., III (1997) *J. Biol. Chem. 272*, 31570−31575.
54. Record, M. T., Jr., Andereson, C. F., and Lohman, T. M. (1978) *Q. Rev. Biophys. 11*, 104−178.
55. Anderson, C. F., Record, M. T., Jr., and Hart, P. A. (1978) *Biophys. Chem. 7*, 301−316.
56. Frank, D. E., Saecker, R. M., Bond, J. P., Capp, M. W., Tsodikov, O. V., Melcher, S. E., Levandoski, M. M., and Record, M. T., Jr. (1997) *J. Mol. Biol. 267*, 1186−1206.
57. Weber, G., and Drickamer, H. G. (1983) *Q. Rev. Biophys. 16*, 89−112.
58. Marky, L. A., and Macgregor, R. B., Jr. (1990) *Biochemistry 29*, 4805−4811.
59. Parsegian, V. A., Rand, R. P., and Rau, D. C. (1995) *Methods Enzymol. 259*, 43−94.
60. deHaseth, P. L., Lohman, T. M., and Records, M. T., Jr. (1977) *Biochemistry 16*, 4783−4790.
61. Lohman, T. L., Overman, L. B., Ferrari, M. E., and Kozlov, A. G. (1996) *Biochemistry 35*, 5272−5279.
62. Koblan, K. S., and Ackers, G. K. (1992) *Biochemistry 31*, 57−65.

BI015572Q